Simulation of Non-Abelian Braiding in Majorana Time Crystals

Raditya Weda Bomantara* and Jiangbin Gong†
Department of Physics, National University of Singapore, Singapore 117543

(Received 8 February 2018; published 7 June 2018)

Discrete time crystals have attracted considerable theoretical and experimental studies but their potential applications have remained unexplored. A particular type of discrete time crystals, termed "Majorana time crystals," is found to emerge in a periodically driven superconducting wire accommodating two different species of topological edge modes. It is further shown that one can manipulate different Majorana edge modes separated in the time lattice, giving rise to an unforeseen scenario for topologically protected gate operations mimicking braiding. The proposed protocol can also generate a magic state that is important for universal quantum computation. This study thus advances the quantum control in discrete time crystals and reveals their great potential arising from their time-domain properties.

DOI: 10.1103/PhysRevLett.120.230405

Introduction.—The idea of time crystals was first coined by Wilczek in 2012 [1]. Despite the existence of a no-go theorem, which prohibits time crystals to arise in the ground state or equilibrium systems [2], time crystals in periodically driven systems, named discrete time crystals (DTCs), have recently attracted considerable interest [3–10]. Two experimental realizations of DTCs have been reported [11,12].

Here we explore the potential applications of DTCs as exotic phases of matter [13]. Specifically, DTCs are exploited to perform topologically protected quantum computation [14,15]. To that end, one needs to first find a particular type of DTC that can simulate non-Abelian, e.g., Ising [14–18] or Fibonacci [14,15,19,20] anyons. Ising anyons can be described in the language of Majorana fermions in one-dimensional (1D) superconducting chains [21–23].

DTCs have recently been proposed in a periodically driven Ising spin chain [8]. As learned from the mapping between 1D superconducting chains and static spin systems [16,24–26], we expect the emergence of DTCs in a periodically driven Kitaev superconducting chain. Indeed, there period-doubling DTCs are obtained using the quantum coherence between two types of topologically protected Floquet Majorana edge modes [27–29]. Such DTCs are termed Majorana time crystals (MTCs) below. Next, a scheme is proposed to physically simulate the non-Abelian braiding of a pair of Majorana fermions [26,30–34] at two different time lattice sites. We also elucidate how our scheme can be used to generate a magic state, which is necessary to perform universal quantum computation [35–39]. These findings open up a new concept in simulating the braiding of Majorana excitations and should stimulate future studies of the applications of DTCs.

Majorana time crystals.—Consider a periodically driven system $H(t)$ of period T. For the first half of each period, $H(t)$ is a 1D Kitaev chain with Hamiltonian $H_1 = \sum_j^{N-1} (-J_j c_{j+1}^\dagger c_j + \Delta_j c_{j+1}^\dagger c_j^\dagger + \text{H.c.}) + \mu_1 \sum_j^N c_j^\dagger c_j$ [22], and for the second half of each period, $H(t) = H_2 = \mu_2 \sum_j^N c_j^\dagger c_j$. Here c_j ($c_j^\dagger$) is the annihilation (creation) operator at site j, J_j and Δ_j are, respectively, the hopping and pairing strength between site j and $j+1$, and μ_1 and μ_2 are the chemical potential at different time steps. Throughout this Letter, we work in a unit system with $\hbar = 1$. Unless otherwise specified later, we take $J_j = J$ and $\Delta_j = \Delta$ for all $j = 1, \ldots, N-1$ for our general discussions. For later use, we also define the one-period propagator $\mathcal{U} = \mathcal{T} \exp(-\int_0^T iH(t')dt')$, where $\mathcal{T}$ is the time ordering operator. One candidate for H_1 is an ultracold atom system [27,29], realizable by optically trapping 1D fermions inside a three-dimensional (3D) molecular Bose-Einstein condensate (BEC). In such an optical lattice setup, the hopping term is already present due to the two Raman lasers generating the optical lattice, while the pairing term can be induced by introducing a radio frequency (rf) field coupling the fermions with Feshbach molecules from the surrounding BEC reservoir. Realizing the periodic quenching between H_1 and H_2 is also possible [27,29].

Our motivation for considering the above model system depicted by $H(t)$ is as follows. If $J = \Delta = \Delta^*$ and $\mu_1 = 0$, then $H(t)$ can be mapped to a periodically driven Ising spin chain [40], which is known to exhibit DTCs [8]. We thus expect $H(t)$ to support DTCs. That is, there exists some observable such that, for a class of initial states, the oscillation in the expectation value of this observable does not share the period of $H(t)$, but exhibits a period of nT, with $n > 1$ being stable against small variations in the system parameters. Furthermore, in the thermodynamic limit, the oscillation of this observable with period nT persists over an infinitely long time.

DTCs in our model emerge from the interplay of periodic driving, hopping, and p-wave pairing. In particular, $H(t)$

yields a number of interesting Floquet topological phases manifested by a varying number of edge modes, with their corresponding eigenphases of $\mathcal{U}$ being 0 or π. These eigenmodes of $\mathcal{U}$ localized at the system edge are often called Floquet zero [27–29] or π edge modes [27,28,48–52], possessing all the essential features of a Majorana excitation [40]. For example, by taking $\mu_2 T = JT = \Delta T = \pi$ and $\mu_1 = 0$, the eigenphases of $\mathcal{U}$ can be explicitly solved, which yield both Majorana zero and π modes. Given that the Majorana zero (π) mode develops an additional phase 0 (π) after one driving period T, a superposition of Majorana zero and π modes will evolve as a superposition, but with their relative phase being π (0) after odd (even) multiples of T. That is, the ensuing dynamics yields period-doubling oscillations for a generic observable. Further, because these edge modes are protected by the underlying topological phase, they do not rely on any fine tuning of the system parameters [40], yielding the necessary robustness for DTCs.

Define two Majorana operators $\gamma_j^A = c_j + c_j^\dagger$ and $\gamma_j^B = i(c_j - c_j^\dagger)$ at each chain site j, with $\gamma_j^A = (\gamma_j^A)^\dagger$, $(\gamma_j^A)^2 = 1$ and similar equalities for γ_j^B, as well as commutation relations $\{\gamma_j^A, \gamma_l^B\} = 2\delta_{AB}\delta_{jl}$. In particular, before the periodic driving is turned on, the choice of system parameters above yield a Majorana zero mode $\Psi(0) = \gamma_1^A$. Once the driving is turned on, $\Psi(0)$ becomes a linear superposition of Majorana zero and π modes and will then evolve nontrivially in time. At time t, it can be written in general as $\Psi(t) = \sum_j \sum_{l=A,B} c_{j,l}(t)\gamma_j^l$, where $\sum_j \sum_{l=A,B} |c_{j,l}(t)|^2 = 1$. To demonstrate how DTCs can be observed in the system, special attention is paid to the quantity $Z(t) = |c_{1,A}(t)|^2 - |c_{1,B}(t)|^2$, which measures the difference between the weight of γ_1^A and γ_1^B in $\Psi(t)$.

Figures 1(a)–1(c) show Z vs time in several cases, whereas Figs. 1(d)–1(f) show the associated subharmonic peak in the power spectrum, defined as $\tilde{Z}(\omega) = \sum_n Z(t)\exp(in\omega T)$. $|\tilde{Z}(\omega)|^2$ is seen to be pinned at $\omega = \pi/T$, confirming the emergence of period-doubling DTCs. Under the special system parameter values chosen above, $\Psi(0)$ comprises an equal-weight superposition of Majorana zero and π modes (shown below) and will therefore undergo period-doubling oscillations between two Majorana operators γ_1^A and γ_1^B as time progresses. As Figs. 1(b) and 1(c) show, tuning the values of μ_1, J, Δ, and μ_2 away from these special values still yields the same period-doubling oscillations for a long timescale, accompanied by some beatings in the time dependence, which diminishes as the system size increases. These results thus justify the term MTC to describe such DTCs.

Simulation of braiding protocol.—Consider now four Majorana modes in our model, labeled as γ_L^A, γ_R^A, γ_L^B, and γ_R^B, with γ_L^A (γ_L^B) and γ_R^A (γ_R^B) representing Majorana edge modes localized in space, at the left and right edges, respectively, and in time, at any even (odd) integer multiple of period.

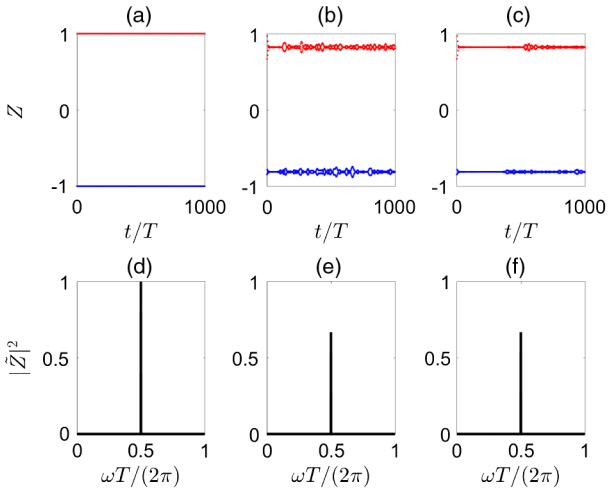

FIG. 1. (a)–(c) Stroboscopic time evolution of Z evaluated at even (red) and odd (blue) integer multiples of T, given that $\Psi(0) = \gamma_1^A$. The system parameters are (a) $\mu_1 T = 0$, $JT = \Delta T = \mu_2 T = \pi$, $N = 50$, (b) $\mu_1 T = 0.1$, $\mu_2 T = 3$, $\Delta T = 1.5JT = 4.2$, $N = 50$, (c) same as (b) but with $N = 200$. (d)–(f) Power spectrum associated with (a)–(c) shows a clear subharmonic peak at $\omega = \pi/T$.

That is, γ_L^B and γ_R^B are obtained by evolving, respectively, γ_L^A and γ_R^A over one period. During our protocol, γ_L^A and γ_L^B will be adiabatically manipulated to simulate braiding, while γ_R^A and γ_R^B are left intact. Such a nonconventional operation is schematically described by Fig. 2. Physical implementation of the adiabatic manipulation in the aforementioned optical-lattice context [27] can be done by slowly tuning the strength of the Raman lasers and the rf field.

Before presenting our protocol, we will first recast H_1 and H_2 in terms of Majorana operators as (focusing on the first three lattice sites and taking $\mu_1 = 0$)

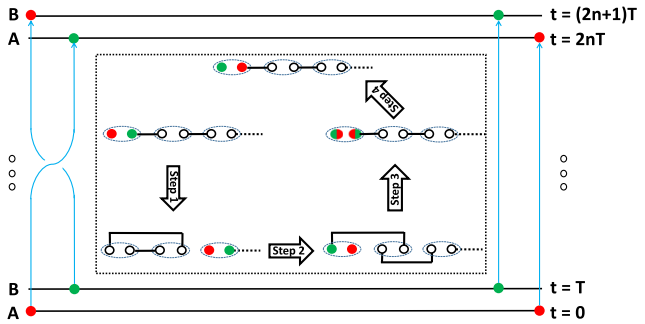

FIG. 2. Because of two nonequivalent time lattice sites labeled A and B, braiding of two left Majorana modes separated in time can be simulated by certain manipulations of the system. (Inset) Details of our protocol. Red and green circles denote the Majorana modes localized at even and odd multiples of of the period, respectively, blue ellipses represent the lattice sites, empty circles denote the rest of the Majorana operators, and black lines denote the coupling between two Majorana modes due to H_1.

$$H_1 = i(\Delta_1/2 - J_1/2)\gamma_1^A\gamma_2^B + i(\Delta_1/2 + J_1/2)\gamma_1^B\gamma_2^A + i\mathrm{Im}(\Delta_2/2 - J_2/2)\gamma_2^A\gamma_3^A + i\mathrm{Re}(\Delta_2/2 + J_2/2)\gamma_2^B\gamma_3^A + i\mathrm{Im}(\Delta_2/2 + J_2/2)\gamma_2^B\gamma_3^B + i\mathrm{Re}(\Delta_2/2 - J_2/2)\gamma_2^A\gamma_3^B + \cdots, \quad (1)$$

and $H_2 = -(\mu_2/2)(1 + i\gamma_1^A\gamma_1^B) + \cdots$, where J_1, Δ_1, J_2, and Δ_2 are subject to adiabatic manipulations, during which J_2 and Δ_2 may be complex, while J_j and Δ_j for $j \neq 2$ are assumed to be always real. For the sake of analytical solutions and better qualitative understandings, we again take $\mu_2 T = J_j T = \Delta_j T = \pi$ at the start to illustrate our idea, so that γ_L^A (γ_L^B), initially prepared from the edge mode of H_1, is precisely γ_1^A (γ_1^B). As demonstrated in Figs. 3(a)–3(c), this fine tuning of the system parameters is not needed in the actual implementation.

In step 1, we exploit the adiabatic deformation of Majorana zero and π modes, denoted $\hat{0}$ and $\hat{\pi}$, along an adiabatic path with $J_2 = \Delta_2$ being real. To develop insights into this step, we parametrize $J_1 + \Delta_1 = 2\pi/T$, $J_1 - \Delta_1 = 2\pi\sin(\phi_1)/T$, $J_2 = \Delta_2 = 2\pi\cos(\phi_1)/T$. As detailed in the Supplemental Material [40], we find (up to an arbitrary overall constant)

$$\hat{0} = [\cos(\phi_1)\gamma_1^A - \sin(\phi_1)\gamma_3^A] + [\cos(\phi_1)\gamma_1^B - \sin(\phi_1)\gamma_3^B];$$
$$\hat{\pi} = [\cos(\phi_1)\gamma_1^A - \sin(\phi_1)\gamma_3^A] - [\cos(\phi_1)\gamma_1^B - \sin(\phi_1)\gamma_3^B].$$

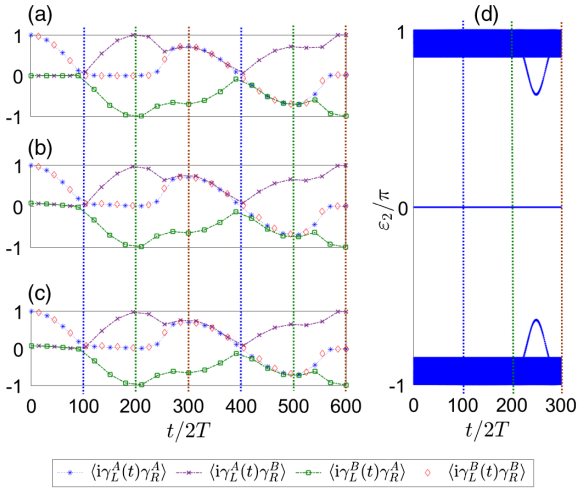

FIG. 3. Time evolution of the Majorana correlation functions during the manipulation process for two different system parameters. Each step takes 200 periods to complete. (a) $\mu_1 T = 0$, $JT = \Delta T = \mu_2 T = \pi$, $N = 100$. (b) $\mu_1 T = 0.3$, $JT = 3.3$, $\Delta T = 2.9$, $\mu_2 T = 3$, $N = 100$. (c) Same as (b) but in the presence of on site, hopping, and pairing disorders, as well as small hopping term in H_2, averaged over 100 disorder realizations. (d) Instantaneous eigenphases (denoted ε_2) of $\mathcal{U}^2$ during steps 1–3, with $\varepsilon_2 = 0$ well separated from the bulk spectrum. Blue, green, and brown vertical dotted lines mark the end of step 1, 2, and 3, respectively.

By tuning ϕ_1 slowly from 0 to $\pi/2$, $\hat{0}$ will adiabatically change from $(\gamma_1^A + \gamma_1^B)$ to $-(\gamma_3^A + \gamma_3^B)$, whereas $\hat{\pi}$ will adiabatically change from $(\gamma_1^A - \gamma_1^B)$ to $(\gamma_3^B - \gamma_3^A)$; i.e., both zero modes and π modes are now shifted to the third site. Because of this adiabatic following, a superposition of $\hat{0}$ and $\hat{\pi}$ modes remains a superposition, thus preserving the DTC feature were the adiabatic process stopped at any time. The net outcome of this step can thus be described simply as $\gamma_1^A \to -\gamma_3^A$ and $\gamma_1^B \to -\gamma_3^B$.

Step 2 continues to adiabatically deform $\hat{0}$ and $\hat{\pi}$. Starting from $J_2 = \Delta_2 = 0$ as a result of step 1, we consider an adiabatic path with $J_2 = -\Delta_2$ being purely imaginary values. If we parametrize $J_1 - \Delta_1 = 2\pi/T$, $J_1 + \Delta_1 = 2\pi\cos(\phi_2)/T$, $J_2 = -\Delta_2 = i\pi\sin(\phi_2)/T$, then one easily finds [40]

$$\hat{0} = [\sin(\phi_2)\gamma_1^B - \cos(\phi_2)\gamma_3^A] - [\sin(\phi_2)\gamma_1^A + \cos(\phi_2)\gamma_3^B];$$
$$\hat{\pi} = [\sin(\phi_2)\gamma_1^B - \cos(\phi_2)\gamma_3^A] + [\sin(\phi_2)\gamma_1^A + \cos(\phi_2)\gamma_3^B].$$

As ϕ_2 adiabatically increases from 0 to $\pi/2$, $\hat{0}$ and $\hat{\pi}$ undergo further adiabatic changes to $(\gamma_1^B - \gamma_1^A)$ and $(\gamma_1^B + \gamma_1^A)$, respectively. The overall transformation of this step is $-\gamma_3^A \to \gamma_1^B$ and $-\gamma_3^B \to -\gamma_1^A$.

In step 3, we exploit further the coherence between Majorana zero and π modes so as to recover the system's original Hamiltonian, while at the same time preventing γ_L^A and γ_L^B from completely untwisting and returning to their original configuration. As an innovative adiabatic protocol, we adiabatically change the system parameters every other period. This amounts to introducing a characteristic frequency π/T in our adiabatic manipulation, resulting in the coupling between zero and π quasienergy space. As the system parameters are adiabatically tuned, Majorana zero and π modes will then adiabatically follow the degenerate eigenmodes of $\mathcal{U}^2$ (i.e., the two-period propagator) associated with zero eigenphase. This leads to a nontrivial rotation between the two Majorana modes dictated by the non-Abelian Berry phase in this degenerate subspace. With this insight, one can envision many possible adiabatic paths to induce a desirable rotation between Majorana 0 and π modes.

After some trial and error attempts, we discover a class of adiabatic paths for step 3 that can yield a rotation of $\pi/4$ between γ_L^A and γ_L^B. Specifically, we fix J_1 and let $\Delta_1 = 2\pi f_{3,a}(t)/T$, $J_2 = \sqrt{2}\pi\exp(i\pi/4)[1 - if_{3,b}(t)]/T$, and $\Delta_2 = \sqrt{2}\pi\exp(-i\pi/4)[1 + if_{3,c}(t)]/T$, where $f_{3,l}(t)$, with $l = a, b, c$ are certain (not necessarily the same) functions that slowly increase from -1 to 1 for every other period. That is, for each new period, $f_{3,l}(t)$ are alternatively increased or stay at the values of the previous step. At the end of the adiabatic manipulation, this step yields the original Hamiltonian, with $\gamma_1^B \to (\gamma_1^A + \gamma_1^B)/\sqrt{2}$ and $-\gamma_1^A \to (\gamma_1^B - \gamma_1^A)/\sqrt{2}$ to a high fidelity.

Finally, in step 4, we repeat the three steps outlined above to obtain the overall transformations $\gamma_L^A \to \gamma_L^B$ and $\gamma_L^B \to -\gamma_L^A$, which completes the simulated braiding operation to the two different species of Majorana modes and at the same time resets the system configuration. As shown in Fig. 2, at the start of the protocol, γ_L^A (γ_L^B) at our MTC appears at even (odd) multiples of T; by contrast, at the end of the protocol, γ_L^A (γ_L^B) appears at odd (even) multiples of T.

To confirm the above analysis, we calculate the evolution of Majorana correlation functions during the manipulation process. The system is assumed to be in the even parity state such that initially $\langle i\gamma_L^A\gamma_R^A\rangle = \langle i\gamma_L^B\gamma_R^B\rangle = 1$ and $\langle i\gamma_L^A\gamma_R^B\rangle = \langle i\gamma_L^B\gamma_R^A\rangle = 0$, where $\gamma_i^\alpha \equiv \gamma_i^\alpha(t=0)$, $\alpha = A, B$, and $i = L, R$. During the manipulation process, $\gamma_A^L(t)$ and $\gamma_B^L(t)$ in general become a superposition of γ_L^A and γ_L^B, thus changing the correlations $\langle i\gamma_L^\alpha(t)\gamma_R^\beta\rangle$, where $\alpha, \beta = A, B$. The success of our protocol is then marked by the final correlation functions $\langle i\gamma_L^A(t_f)\gamma_R^A\rangle = \langle i\gamma_L^B(t_f)\gamma_R^B\rangle = 0$ and $\langle i\gamma_L^A(t_f)\gamma_R^B\rangle = -\langle i\gamma_L^B(t_f)\gamma_R^A\rangle = 1$. In experiment, Majorana correlation functions $\langle i\gamma_L^A\gamma_R^A\rangle$ and $\langle i\gamma_L^B\gamma_R^B\rangle$ may be measured via a time-of-flight imaging method, as proposed in Ref. [53], or indirectly by measuring the parity of the wire [54] at even and odd integer multiples of T. To measure cross-correlation functions such as $\langle i\gamma_L^B\gamma_R^A\rangle$, one could first turn off the periodic driving on the right half of the wire after the protocol is completed, then wait for one period. Since γ_R^A is a Majorana zero mode in the absence of periodic driving by construction, it will stay invariant in one period, whereas the left Majorana mode will transform into γ_L^B [55]. The same read-out process can then be carried out to measure their correlation functions.

The full evolution of Majorana correlation functions is depicted in Figs. 3(a)–3(c) under different system parameter values. In particular, Fig. 3(c) assumes also the presence of disorders and a small hopping term in H_2, which may arise due to the presence of the Raman lasers, even after taking low frequency and large detuning values. More precisely, hopping, pairing, and on site static disorders are considered by taking $J_j = J + \delta J_j$, $\Delta_j = \Delta + \delta\Delta_j$, $\mu_1 \to \mu_1 + \delta\mu_{1,j}$, and $\mu_2 \to \mu_2 + \delta\mu_{2,j}$, where $\delta J_j T$, $\delta\Delta_j T$, $\delta\mu_{1,j}T$, and $\delta\mu_{2,j}T$ uniformly take random values between -0.1 and 0.1, while the small hopping term is of the form $-\sum_j(\mathcal{J} + \delta\mathcal{J}_j)c_{j+1}^\dagger c_j + \text{H.c.}$, where $\mathcal{J}T = 0.025$ and $\delta\mathcal{J}_j T \in [-0.01, 0.01]$. The fact that Figs. 3(a)–3(c) look qualitatively the same demonstrates the robustness of our protocol against such system imperfections. Finally, plotted in Fig. 3(d) is the whole eigenphase spectrum of $\mathcal{U}^2$, which indicates that its zero eigenphases are well separated from the rest of the spectrum, thus confirming the topological protection needed to realize the rotation between γ_L^A and γ_L^B.

Discussion.—Because of fermion parity conservation, a minimum of four Majorana modes is required to harness their non-Abelian features for nontrivial (single-qubit) gate operations. This Letter demonstrates, through exploiting the time-domain features, that this can be achieved in a minimal single wire setup, thus avoiding the necessity to design complicated geometries [30,31,33,34]. Moreover, as demonstrated in the Supplemental Material [40], our setup can be readily extended to an array of wires to simulate more intricate braiding between various pairs of Majorana modes at different times and wires. In view of these two aspects, it is expected that certain quantum computational tasks may now be carried out using significantly less number of wires.

As another feature of the proposed protocol, the end of step 3 has achieved the transformation $\gamma_L^A \to (1/\sqrt{2})(\gamma_L^A + \gamma_L^B)$ and $\gamma_L^B \to (1/\sqrt{2})(\gamma_L^B - \gamma_L^B)$, which can be written as $V = \exp[-(\pi/8)\gamma_L^A\gamma_L^B]$. In the even parity subspace, a qubit can be encoded in the common eigenstates of the parity operators $i\gamma_L^A\gamma_R^A$ and $i\gamma_L^B\gamma_R^B$, such that $i\gamma_L^A\gamma_R^A|0\rangle = i\gamma_L^B\gamma_R^B|0\rangle = |0\rangle$ and $i\gamma_L^A\gamma_R^A|1\rangle = i\gamma_L^B\gamma_R^B\rangle|1\rangle = -|1\rangle$. It can be easily verified that V maps $|0\rangle$ to a magic state $\cos(\pi/8)|0\rangle - \sin(\pi/8)|1\rangle$. It is known that a combination of Clifford gates and a magic state is required to achieve universal quantum computation [35,36]. While Clifford gates can be realized in a typical Ising anyonic model alone, the creation of a magic state normally requires an additional dynamical process [37–39]. The rather straightforward realization of the operation V here is hence remarkable.

It is also important to ask to what extent the gate operations here share the robustness of the braiding of two Majorana modes. On the one hand, if J_2, Δ_1, and Δ_2 in step 3 take arbitrary time dependence then the desired braiding outcome cannot be achieved. On the other hand, to physically implement a braiding operation without the use of direct spatial interchange between two Majorana modes, we expect some necessary control to restrict the time dependence of J_2, Δ_1, and Δ_2 used in step 3 to a certain degree. Our further investigations [40] indicate that our protocol does enjoy some weak topological protection, in the sense that its fidelity is rather stable under considerable time-dependent deformation: $J_2 \to J_2 + \delta J_2$, $\Delta_1 \to \Delta_1 + \delta\Delta_1$, and $\Delta_2 \to \Delta_2 + \delta\Delta_2$ in step 3, where δJ_2, $\delta\Delta_1$, and $\delta\Delta_2$ represent time-dependent perturbations, vanishing at the start and end of step 3, with relative strength on the order of 5% [40].

Conclusion.—A coherent superposition of Majorana zero and π modes of a periodically driven 1D superconducting wire is shown to yield period-doubling MTCs. By adiabatic manipulation of the Majorana zero and π modes, we have proposed a relatively robust scheme to mimic the braiding of two Majorana modes localized at different physical and time lattice sites. Our approach is promising for physical resource saving. As an important side result, we also obtain a magic state crucial for universal quantum computation [35,36].

J. G. is supported by the Singapore NRF Grant No. NRF-NRFI2017-04 (WBS No. R-144-000-378-281) and by the Singapore Ministry of Education Academic Research Fund Tier I (WBS No. R-144-000-353-112).

*phyrwb@nus.edu.sg
†phygj@nus.edu.sg

[1] F. Wilczek, Phys. Rev. Lett. **109**, 160401 (2012).
[2] H. Watanabe and M. Oshikawa, Phys. Rev. Lett. **114**, 251603 (2015).
[3] K. Sacha, Phys. Rev. A **91**, 033617 (2015).
[4] D. V. Else, B. Bauer, and C. Nayak, Phys. Rev. Lett. **117**, 090402 (2016).
[5] N. Y. Yao, A. C. Potter, I.-D. Potirniche, and A. Vishwanath, Phys. Rev. Lett. **118**, 030401 (2017).
[6] W. W. Ho, S. Choi, M. D. Lukin, and D. A. Abanin, Phys. Rev. Lett. **119**, 010602 (2017).
[7] D. V. Else, B. Bauer, and C. Nayak, Phys. Rev. X **7**, 011026 (2017).
[8] B. Huang, Y.-H. Wu, and W. V. Liu, Phys. Rev. Lett. **120**, 110603 (2018).
[9] A. Russomanno, F. Iemini, M. Dalmonte, and R. Fazio, Phys. Rev. B **95**, 214307 (2017).
[10] A. Russomanno, B. E. Friedman, and E. G. Dalla Torre, Phys. Rev. B **96**, 045422 (2017).
[11] J. Zhang, P. W. Hess, A. Kyprianidis, P. Becker, A. Lee, J. Smith, G. Pagano, I.-D. Potirniche, A. C. Potter, A. Vishwanath, N. Y. Yao, and C. Monroe, Nature (London) **543**, 217 (2017).
[12] S. Choi, J. Choi, R. Landig, G. Kucsko, H. Zhou, J. Isoya, F. Jelezko, S. Onoda, H. Sumiya, V. Khemani, C. v. Keyserlingk, N. Y. Yao, E. Demler, and M. D. Lukin, Nature (London) **543**, 221 (2017).
[13] K. Sacha and J. Zakrewski, Rep. Prog. Phys. **81**, 016401 (2018).
[14] C. Nayak, S. H. Simon, A. Stern, M. Freedman, and S. Das Sarma, Rev. Mod. Phys. **80**, 1083 (2008).
[15] V. Lahtinen and J. K. Pachos, SciPost Phys. **3**, 021 (2017).
[16] A. Kitaev, Ann. Phys. (Amsterdam) **321**, 2 (2006).
[17] A. Ahlbrecht, L. S. Georgiev, and R. F. Werner, Phys. Rev. A **79**, 032311 (2009).
[18] G. Moore and N. Read, Nucl. Phys. **B360**, 362 (1991).
[19] S. Trebst, M. Troyer, Z. Wang, and A. W. W. Ludwig, Prog. Theor. Phys. Suppl. **176**, 384 (2008).
[20] R. S. K. Mong, D. J. Clarke, J. Alicea, N. H. Lindner, P. Fendley, C. Nayak, Y. Oreg, A. Stern, E. Berg, K. Shtengel, and M. P. A Fisher, Phys. Rev. X **4**, 011036 (2014).
[21] D. A. Ivanov, Phys. Rev. Lett. **86**, 268 (2001).
[22] A. Y. Kitaev, Phys. Usp. **44**, 131 (2001).
[23] M. Stone and S.-B Chung, Phys. Rev. B **73**, 014505 (2006).
[24] P. Fendley, J. Stat. Mech. (2012) P11020.
[25] F. L. Pedrocchi, S. Chesi, S. Gangadharaiah, and D. Loss, Phys. Rev. B **86**, 205412 (2012).
[26] Y.-C. He and Y. Chen, Phys. Rev. B **88**, 180402(R) (2013).
[27] L. Jiang, T. Kitagawa, J. Alicea, A. R. Akhmerov, D. Pekker, G. Refael, J. I. Cirac, E. Demler, M. D. Lukin, and P. Zoller, Phys. Rev. Lett. **106**, 220402 (2011).
[28] Q.-J. Tong, J.-H. An, J. B. Gong, H.-G. Luo, and C. H. Oh, Phys. Rev. B **87**, 201109(R) (2013).
[29] D. E. Liu, A. Levchenko, and H. U. Baranger, Phys. Rev. Lett. **111**, 047002 (2013).
[30] J. Alicea, Y. Oreg, G. Refael, F. von Oppen, and M. P. A. Fisher, Nat. Phys. **7**, 412 (2011).
[31] B. van Heck, A. R. Akhmerov, F. Hassler, M. Burrello, and C. W. J. Beenakker, New J. Phys. **14**, 035019 (2012).
[32] C. V. Kraus, P. Zoller, and M. A. Baranov, Phys. Rev. Lett. **111**, 203001 (2013).
[33] T. Karzig, F. Pientka, G. Refael, and F. von Oppen, Phys. Rev. B **91**, 201102 (2015).
[34] P. Gorantla and R. Sensarma, arXiv:1712.00453 [Phys. Rev. B (to be published)].
[35] T. Karzig, Y. Oreg, G. Refael, and M. H. Freedman, Phys. Rev. X **6**, 031019 (2016).
[36] S. Bravyi and A. Kitaev, Phys. Rev. A **71**, 022316 (2005).
[37] S. Bravyi, Phys. Rev. A **73**, 042313 (2006).
[38] M. Freedman, C. Nayak, and K. Walker, Phys. Rev. B **73**, 245307 (2006).
[39] P. Bonderson, D. J. Clarke, C. Nayak, and K. Shtengel, Phys. Rev. Lett. **104**, 180505 (2010).
[40] See Supplemental Material at http://link.aps.org/supplemental/10.1103/PhysRevLett.120.230405 for more details about our protocol, and its extension to an array of quantum wires, and mapping between spin and superconducting lattice, formulation of Floquet Majorana modes and MTCs, which includes Refs. [41–47].
[41] J. H. Shirley, Phys. Rev. **138**, B979 (1965).
[42] H. Sambe, Phys. Rev. A **7**, 2203 (1973).
[43] T. Oka and H. Aoki, Phys. Rev. B **79**, 081406 (2009).
[44] N. H. Lindner, G. Refael, and V. Galitski, Nat. Phys. **7**, 490 (2011).
[45] E. Knill, Nature (London) **434**, 39 (2005).
[46] C. J. Ballance, T. P. Harty, N. M. Linke, M. A. Sepiol, and D. M. Lucas, Phys. Rev. Lett. **117**, 060504 (2016).
[47] N. Lang and H. P. Büchler, SciPost Phys. **4**, 007 (2018).
[48] D. Y. H. Ho and J. B. Gong, Phys. Rev. B **90**, 195419 (2014).
[49] L. W. Zhou, H. L. Wang, D. Y. H. Ho, and J. B. Gong, Eur. Phys. J. B **87**, 204 (2014).
[50] R. W. Bomantara, G. N. Raghava, L. W. Zhou, and J. B. Gong, Phys. Rev. E **93**, 022209 (2016).
[51] M. N. Chen, F. Mei, W. Shu, H.-Q. Wang, S.-L. Zhu, L. Sheng, and D. Y. Xing, J. Phys. Condens. Matter **29**, 035601 (2017).
[52] H.-Q. Wang, M. N. Chen, R. W. Bomantara, J. B. Gong, and D. Y. Xing, Phys. Rev. B **95**, 075136 (2017).
[53] C. V. Kraus, S. Diehl, M. A. Baranov, and P. Zoller, New J. Phys. **14**, 113036 (2012).
[54] J. F. Sherson, C. Weitenberg, M. Endres, M. Cheneau, I. Bloch, and S. Kuhr, Nature (London) **467**, 68 (2010).
[55] This exchange $\gamma_L^A \leftrightarrow \gamma_L^B$ is trivial as compared with the braiding exchange $\gamma_L^A \rightarrow \gamma_L^B$ and $\gamma_L^B \rightarrow -\gamma_L^A$ (i.e., an extra negative sign is necessary for a braiding process).